SEISMIC NOISE ATTENUATION BY TIME-FREQUENCY PEAK FILTERING BASED ON BORN-JORDAN DISTRIBUTION

YUHAN LIU, ZHENMING PENG, YUQING WANG and YANMIN HE

School of Information and Communication Engineering, Center for Geoscience Information, University of Electronic Science and Technology of China, Chengdu 610054, P.R. China. zmpeng@uestc.edu.cn

(Received November 24, 2017; revised version accepted October 6, 2018)

ABSTRACT

Liu, Y., Peng, Z.M., Wang, Y.Q. and He, Y.M., 2018. Seismic noise attenuation by time-frequency peak filtering based on Born-Jordan distribution. *Journal of Seismic Exploration*, 27: 557-575.

The signal-to-noise ratio (SNR) improvement of seismic signals is an important step in seismic exploration. A time-frequency peak filtering based on Born-Jordan distribution (BJD-TFPF) algorithm is proposed in this paper. Time-frequency peak filtering (TFPF) is an effective filtering method for signal enhancement. The Born-Jordan distribution (BJD) has a good balance between suppressing cross terms and maintaining time-frequency aggregation. This algorithm takes advantage of TFPF and BJD to reduce noise while preserving the signal. In this paper, we also discuss different factors affecting the BJD-TFPF in terms of improving the practicality. The proposed method is applied to synthetic records and real seismic data. The results show that this algorithm can recover the signal effectively and is suitable for the filtering of seismic data. The results also reveal the effects of various factors on the practicality of the BJD-TFPF .

KEY WORDS: time-frequency peak filtering, seismic signal, Born-Jordan distribution, variable factors.

INTRODUCTION

Seismic noise suppression plays an important role in seismic data processing to improve the signal-to-noise ratio (SNR) of seismic data (Lin et al., 2013). Signals with low SNR will have negative impact on seismic imaging and explanation. Therefore, many algorithms have been developed

0963-0651/18/$5.00

to eliminate noise. Jones and Levy (1987) suppressed noise by Karhunen-Loéve transform, and White (1984) applied spectral coherence methods in seismic data estimation. Time-frequency peak filtering (TFPF), based on time-frequency analysis (Arnold et al., 1993), is an effective method to suppress noise (Mesbah and Boashash, 2001). This approach can recover the signal with additive white Gaussian noise (WGN) and quaternary frequency shift keying (4FSK) (Boashash and Mesbah, 2004). The algorithm shows that a very clean recovery of signals can be accomplished for SNR as low as -9 dB (Boashash and Mesbah, 2004). Then, the TFPF is used to reduce the random noise of seismic signals. In order to increase the linearity of a signal in practical processing, many researchers have applied Pseudo Wigner-Ville distribution (PWVD) to linearize instantaneous frequency (IF) (Li et al., 2013; Liu et al., 2014; Wang et al., 2013; Liu et al., 2014; Lin et al., 2011). Considering the correlation between traces, spatial-trace and parabolic-trace can improve the linearity of a signal and can be well adapted to the actual changes of the seismic trace (Lin et al., 2014; Tian and Li, 2014). Taking the spatial correlation of the reflection events between adjacent channels in different layers into account, Xiong et al. (2014) proposed a novel method for TFPF along the local direction of the reflection event instead of along the channel (Xiong et al., 2014). Joint time-frequency distribution is used to reduce the effects of the interferences and enhance the energy concentration around the IF of the signal in the time-frequency domain (Zhang et al., 2013). Other methods, like the nonlinearity approach (Lin et al., 2013) and spatiotemporal TFPF (Liu et al., 2013) have been proposed to improve the TFPF algorithm as well. Although there are different optimizations of TFPF, most of them choose PWVD, or are based on PWVD, to enhance the linearity.

PWVD belongs to Cohen's time-frequency distribution, which is an extension algorithm of Wigner-Ville distribution (WVD). Adding different window functions to WVD, Cohen's time-frequency distribution has many different forms to eliminate cross terms. However, the time-frequency resolution decreases while the cross terms are removed. Among Cohen's time-frequency distribution, Born-Jordan distribution (BJD) preserves the time-frequency resolution well when removing cross terms. Compared with PWVD, the Born-Jordan distribution (BJD) has better time-frequency aggregation. Hence, we propose a TFPF based on Born-Jordan distribution (BJD-TFPF) in this paper. The kernel function of BJD is an ideal low-pass function, which can suppress cross terms. To show its performance, we compare the SNR of the PWVD-TFPF and the BJD-TFPF, through experiments on multicomponent signal, synthetic seismic data and field data. Furthermore, we give different window lengths and discuss the relationship between window length and SNR of synthetic seismic data to apply this method practically. The results show that the BJD method performs well in SNR, peak signal-to-noise ratio (PSNR) and mean square error (MSE). The results also show the influence of various factors on the performance of the BJD-TFPF.

TFPF WITH BORN-JORDAN DISTRIBUTION

In this section, we describe the BJD-TFPF briefly. Cohen's time-frequency distribution of signal $x(t)$ can be written as (Ivanovic, 2003)

$$C_x(t,f:g)=\iint A_x(\theta,\tau)g(\theta,\tau)e^{-j(\theta t+f\tau)}d\tau d\theta \quad , \tag{1}$$

where $A_x(\theta,\tau)$ is the ambiguity function of signal $x(t)$ defined as

$$A_x(\theta,\tau)=\frac{1}{2\pi}\int x(u+\frac{\tau}{2})x^*(u-\frac{\tau}{2})e^{ju\theta}du \quad , \tag{2}$$

and $g(\theta,\tau)$ is the kernel function defined in ambiguity domain (θ,τ)(τ represents the time delay, θ represents the frequency shift called Doppler) which is 2D Fourier transform of smoothing function in time-frequency domain, and * is the conjugate operator. The weighting function, $g(\theta,\tau)$, acts to maintain the signal and reduce the interference term. For example, if $g(\theta,\tau)$=1, we get WVD. The kernel function of PWVD is $g(\theta,\tau)$=H(f), where H(f) is the Fourier transform of rectangle window $h(t)$. However, PWVD loses some properties with this kernel. The kernel function of BJD

$$g(\theta,\tau)=\frac{\sin(\pi\theta\tau)}{\pi\theta\tau} \quad . \tag{3}$$

$g(\theta,\tau)$ is a two-dimensional Sinc function in the (θ,τ) plane that can smooth both in the time domain and the frequency domain compared with PWVD which only can smooth in the frequency domain. Furthermore, we can change the degree of smoothing to change its performance and it can suppress the cross terms in time-frequency distribution. PWVD can ~~also~~ suppress cross terms as well but without marginal condition and frequency support properties, while BJD preserves these properties. The class of signals considered in this paper can be modeled as (Boashash and Mesbah, 2004)

$$s(t)=x(t)+n(t)=\sum_{k=1}^{p}x_k(t)+n(t) \quad , \tag{4}$$

where $n(t)$ is an additive noise, and $x_k(t)$ is a bandlimited nonstationary deterministic component with overlapping frequency spectra. We hope to recover signal $x(t)$ from the observation signal $s(t)$.

With frequency-coded modulation, we can get the analytic signal (Boashash and Mesbah, 2004)

$$z(t) = e^{j2\pi\mu\int_0^t s(\lambda)d\lambda} \quad , \tag{5}$$

where μ is the conversion factor.

The BJD of the analytic signal is defined as

$$W_z(t,f) = \frac{1}{2a}\int\frac{1}{\tau}e^{-jf\tau}\int_{t-a\tau}^{t+a\tau} z(u+\frac{\tau}{2})z^*(u-\frac{\tau}{2})e^{-jf\tau}dud\tau \quad , \tag{6}$$

where * denotes the conjugate operator. The IF estimation is obtained by maximizing the BJD over frequency, that is (Boashash and Mesbah, 2004)

$$f_z(t) = \arg\max_f[W_z(t,f)] \quad , \tag{7}$$

where $\arg\max_f[\cdot]$ represents finding the frequency related to the max value in TFD.

Supposing that the observed seismic signal with noise is $s(t)$, the steps for the iterative BJD-TFPF are as follows:

Step one: Encode and scale the noisy signal with the unit amplitude and the unit conversion factor (Boashash and Mesbah, 2004).

Step two: Apply BJD to the coded analytic signal and find the IF.

Step three: Process every trace to get complete filtered seismic data.

EXPERIMENT ON SIMULATED AND REAL DATA

Multicomponent Signal

First, we consider a multicomponent signal

$$x(t) = \begin{cases} 0.8\sin(0.04t + 3.75\times10^{-4}t\sin(0.000625t)) \\ +\sin(0.01875t) + \sin(0.06t), 0 \le t \le 512 \\ 0.8\sin(0.04t + 3.75\times10^{-4}t\sin(0.000625t)) \\ +2(1-\frac{t}{1024})\sin(0.01875t + 2.75\times10^{-11}(t-512)^3) \\ +\sin(0.06t), 512 \le t \le 1024 \end{cases} . \tag{8}$$

Random noise with mean 0 and variance 1 is added to test for traditional PWVD-TFPF and BJD-TFPF. Time window length is 5 (sample point), while frequency window length is 7. After three iterations, the results are shown in Fig. 1. SNR, PSNR and MSE are calculated as

$$snr=10\times\log(\frac{Ps}{Pn}) \quad , \tag{9}$$

where *Ps* denotes the effective power of the original signal and *Pn* means the effective power of the noisy signal. Furthermore,

$$\text{mse}=\frac{1}{m}\times\sum_{i=1}^{m}\left\|X(i)-S(i)\right\|^2 \quad , \tag{10}$$

and

$$psnr=10\times\log\left[\frac{(\max(X))^2}{mse}\right] \quad , \tag{11}$$

where X and S represents the original signal and the filtered signal, respectively.

From Fig. 1 we can see that both methods can suppress noise well but BJD-TFPF performs better at the boundaries, which illustrates that BJD has good marginal properties so it can preserve margins and improve SNR. SNR, PSNR and MSE are listed in Table 1. As seen from Table 1, BJD-TFPF can improve SNR and PSNR by about 3 dB. It can also reduce MSE compared with PWVD-TFPF.

Table 1. Comparisons of SNR, PSNR and MSE of TFPF and BJD-TFPF [A]

Indicators	PWVD	BJD
SNR(dB) before filtering	0.8688	0.8688
SNR(dB) after filtering	7.9758	**11.6947**
SNR(dB) (improvement)	7.1070	**10.8259**
PSNR(dB) after filtering	10.8332	**14.5521**
MSE after filtering	0.1876	**0.0797**

[A.] In random noise condition with SNR≈0.9dB

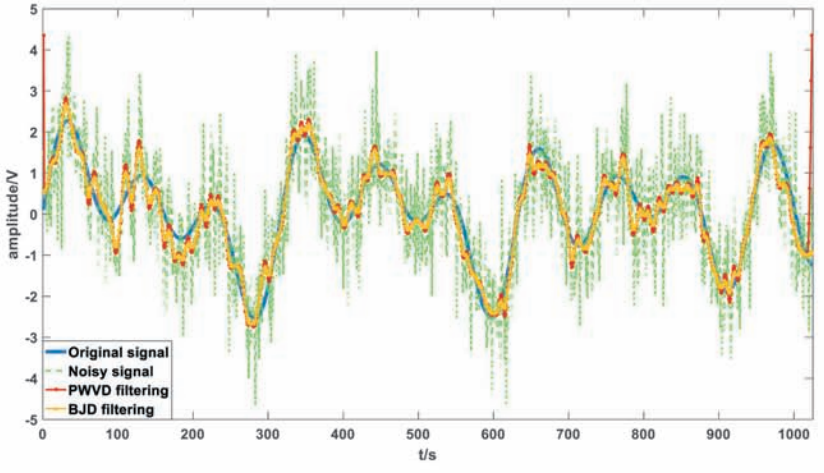

(a)

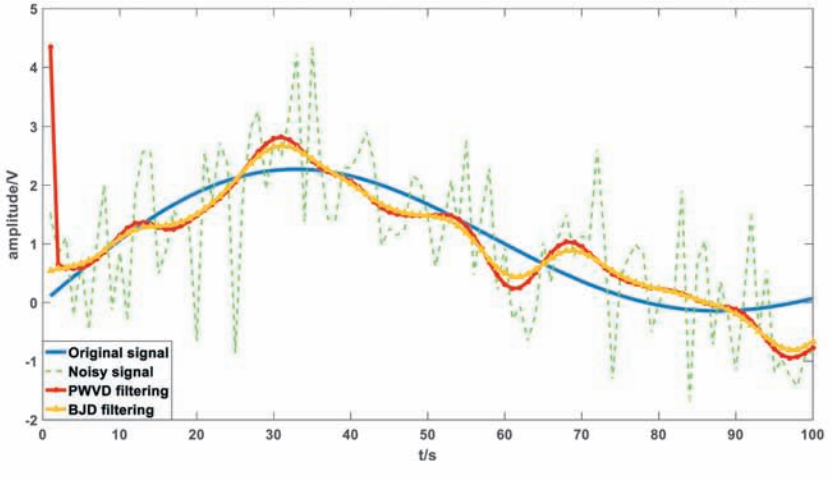

(b)

Fig. 1. Filtering results of multicomponent signal with random noise. (a) Filtering results. (b) Partial enlarged detail.

Then, WGN is added to the signal with SNR = –9dB. Other parameters are the same as before and the results are displayed in Fig. 2.

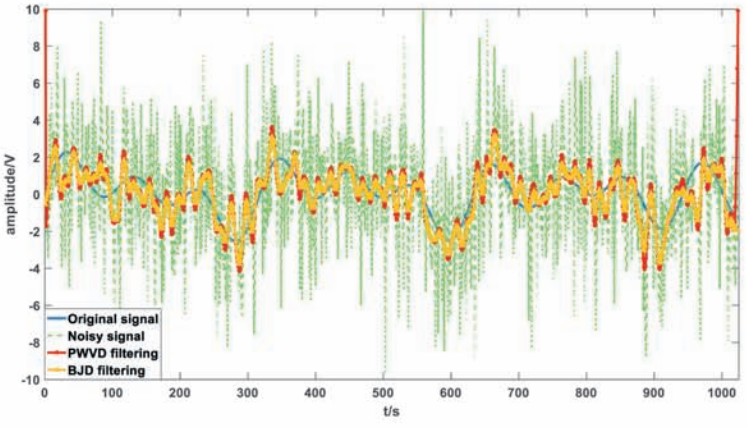

(a)

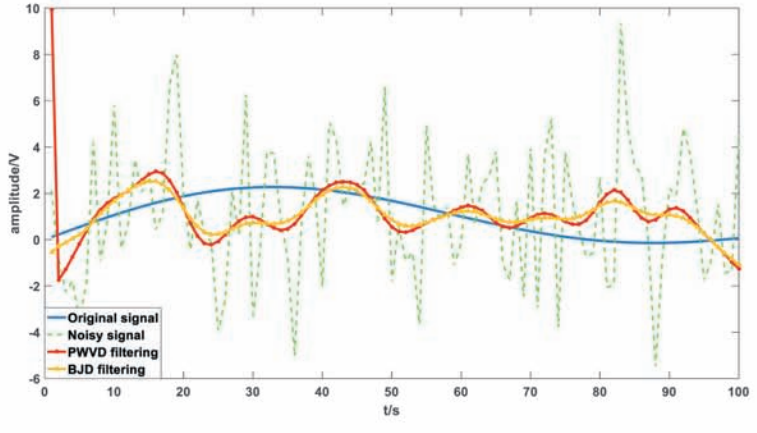

(b)

Fig. 2. Filtering results of multicomponent signal with WGN. (a) Filtering results. (b) Partial enlarged detail.

Fig. 2 also shows that PWVD-TFPF and our method can recover the original signal well in strong noise conditions. However, BJD-TFPF can maintain signal without many fluctuations. Fig. 2 displays the marginal property of BJD as well, which causes the improvement of SNR. The related results are displayed in Table 2, which shows that BJD-TFPF performs better not only in SNR but also in PSNR. Moreover, BJD-TFPF can decrease MSE as well. We can see that our method can increase SNR by 2dB because it preserves the margin of the signal and decreases MSE by 46%.

Table 2. Comparisons of SNR, PSNR and MSE of TFPF and BJD-TFPF[A]

Indicators	PWVD	BJD
SNR(dB) before filtering	-8.9848	-8.9848
SNR(dB) after filtering	-0.3783	**2.3167**
SNR(dB) (improvement)	8.6065	**11.3015**
PSNR(dB) after filtering	2.4791	**5.1741**
MSE after filtering	1.2841	**0.6904**

[A.] In WGN condition with SNR = -9dB

This paper also compares the performance of PWVD and BJD filtering on the SNR and MSE, as depicted in Fig. 3. Fig. 3 shows the varying curves of SNR and MSE after filtering with different SNR of WGN. It can be concluded that in different SNR conditions, BJD-TFPF can obtain smaller MSE, which means this method can maintain a stable signal. BJD-TFPF also gives a better SNR in different conditions.

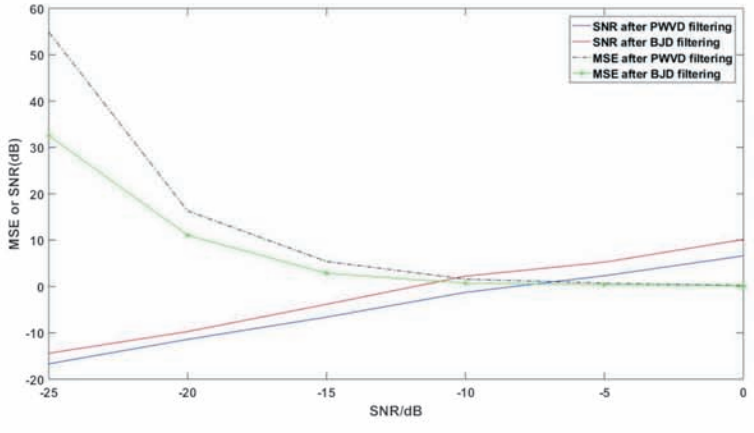

Fig. 3. Comparison of relationship between SNR and MSE of multicomponent signal with two methods.

Synthetic seismogram

To verify the de-noising performance of BJD-TFPF, a 40-trace synthetic seismogram is generated by a series of reflection coefficients convolved with a 30 Hz Ricker wavelet, as shown in Fig. 4(a). The data contains 1000 points with a sampling interval of 2 ms. In addition, the time-domain window length is 7, while the frequency-domain window length is 9. We first test signal with random noise (mean = 0, variance = 0.25) and the result is shown in Fig. 4.

Fig. 4 shows that the original signal is flooded in noise. From Fig. 4, we can see that both methods can suppress noise. Compared with PWVD-TFPF, the proposed method can reduce more noise because of its marginal property. We show the 15th trace of the original signal and the filtered signal by two methods in Fig. 5. Fig. 5 displays the waveform of the seismic signal with PWVD and BJD, which illustrates that both methods can suppress noise well. In terms of recovering signal, these two approaches achieve competitive performance but the same phase axis is recovered. Some indicators are recorded in Table 3.

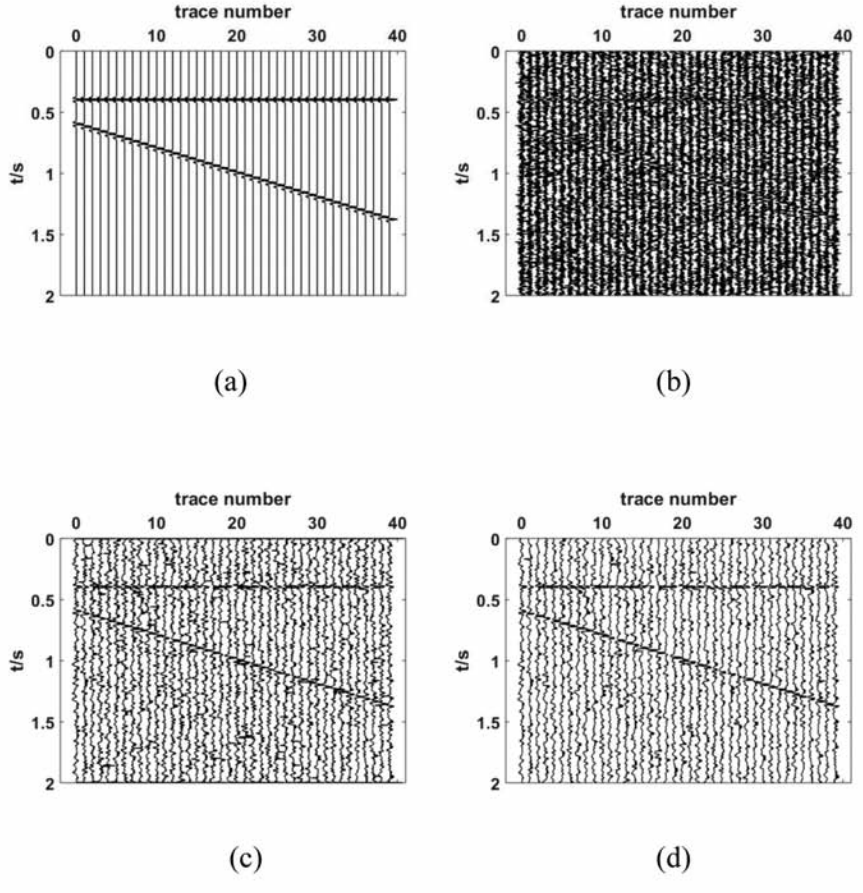

Fig. 4. Filtering results of synthetic seismogram with random noise. (a) Original 40 trace data. (b) Noisy seismic data. (c) PWVD-TFPF result. (d) BJD-TFPF result.

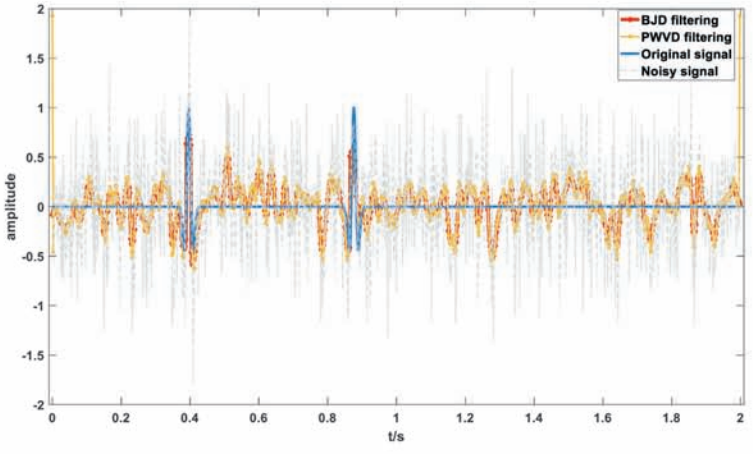

Fig. 5. 15th trace of the seismic signal.

Table 3. Comparisons of SNR, PSNR and MSE of 40 traces of seismic data[A]

Indicators	PWVD	BJD
SNR(dB) before filtering	-13.9865	-13.9865
SNR(dB) after filtering	-6.3389	**-4.6860**
SNR(dB) (improvement)	7.6476	**9.3005**
PSNR(dB) after filtering	13.6726	**15.3255**
MSE after filtering	0.0429	**0.0293**

[A] In random noise condition with SNR ≈ -13dB

Table 3 shows the improvement of SNR by our method is 1.65 dB and MSE reduces by about 31%, illustrating that our method performs better. To verify the effectiveness of the two methods, we then add WGN (SNR = -9dB). The results are depicted in Fig. 6. From Fig. 6 we can see that both methods can recover a signal and the proposed method shows a clearer signal because it can preserve the signal margin. As before, no matter BJD-TFPF or PWVD-TFPF, the same phase axis is recovered clearly. We also show the 15th trace of the original and the filtered signal with PWVD and BJD in Fig. 7. From Fig. 7(a) we can see that both approaches can attenuate noise. Fig. 7(b) illustrates that the two methods can preserve an effective signal in a WGN condition compared with a random noise situation. To show it clearly, we change the color of the lines. Furthermore, as seen in Fig. 7(b), our method performs well without salient noise, as shown in the black circle. Indicators are shown in Table 4. Table 4 illustrates that our method can increase SNR by about 1.8 dB and PSNR by 1.9 dB. MSE reduces by about 35% with BJD-TFPF as well.

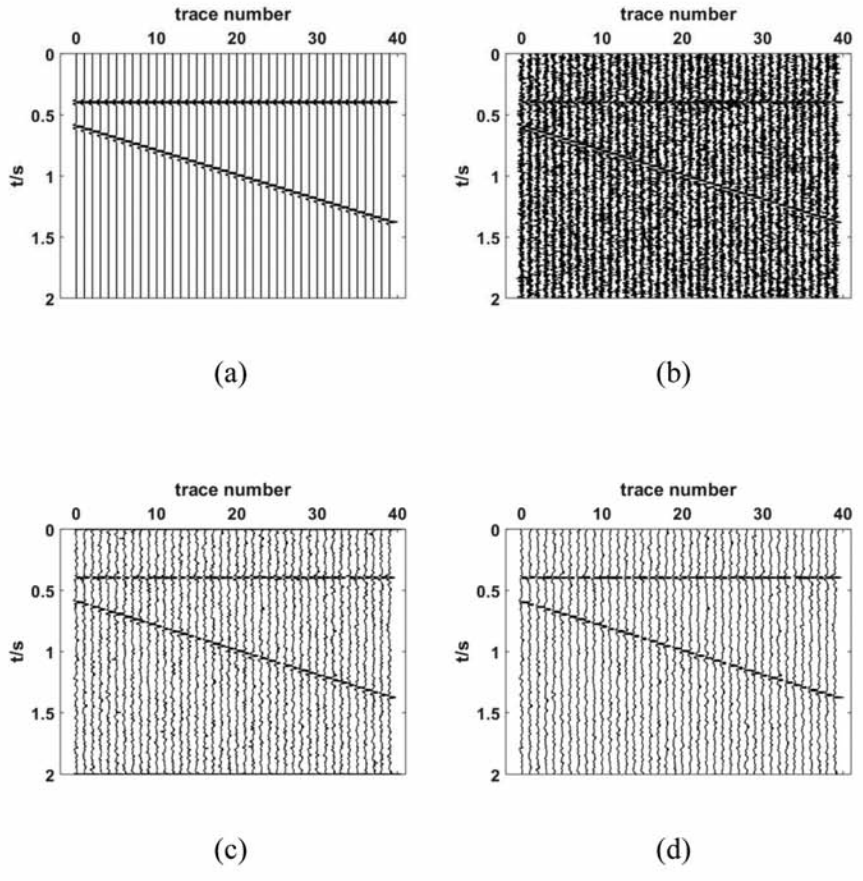

Fig. 6. Filtering results of the synthetic seismogram with WGN. (a) Original 40-trace data. (b) Noisy seismic data. (c) PWVD-TFPF result. (d) BJD-TFPF result.

Table 4. Comparisons of SNR, PSNR and MSE of 40-trace seismic data [A]

Indicators	PWVD	BJD
SNR(dB) before filtering	-8.9278	-8.9278
SNR(dB) after filtering	-1.9338	**-0.0727**
SNR(dB) (improvement)	6.9940	**8.8551**
PSNR(dB) after filtering	18.0777	**19.9388**
MSE after filtering	0.0156	**0.0101**

[A.] In WGN condition with SNR= -9dB

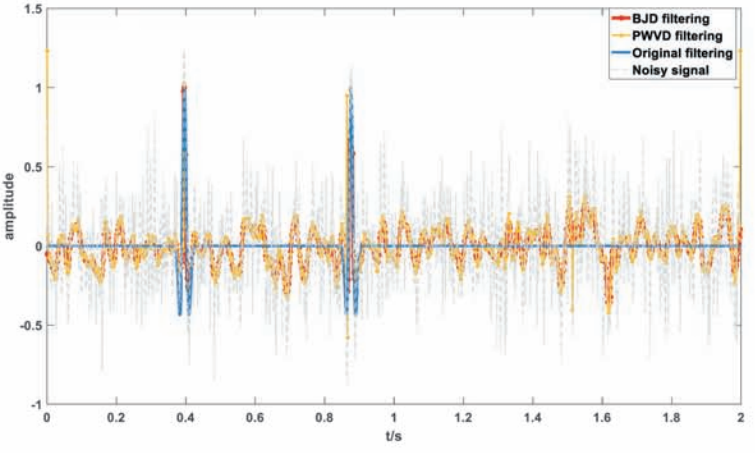

(a)

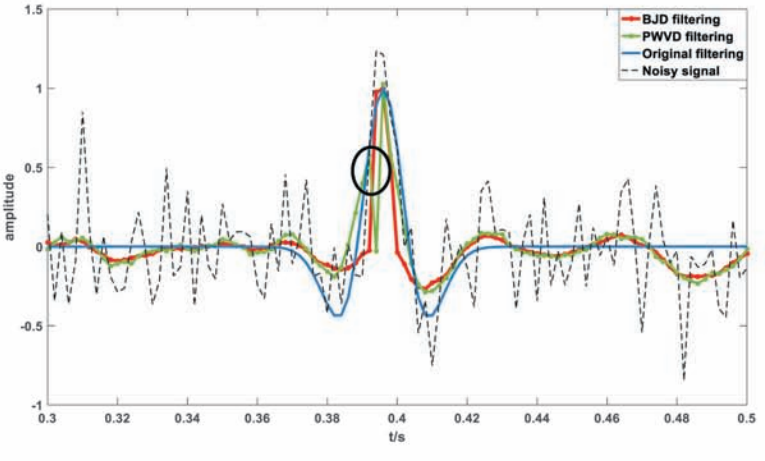

(b)

Fig. 7. 15th trace of the seismic signal. (a) Whole result. (b) Partial detail.

Real seismic data

To test the practicality of the proposed BJD-TFPF method, we apply our method to real seismic data acquired by 250 Hz sampling frequency and recorded every 5 seconds. Taking only 300 traces of the data, we set the time-domain window length to 7, and the frequency-domain window length to 3. The results after one iteration are pictured in Fig. 8.

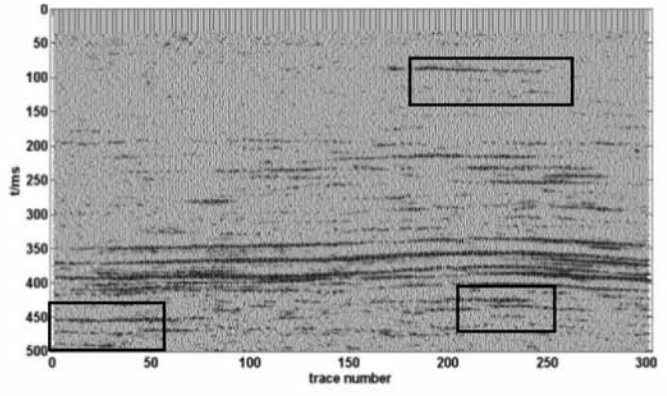

(a)

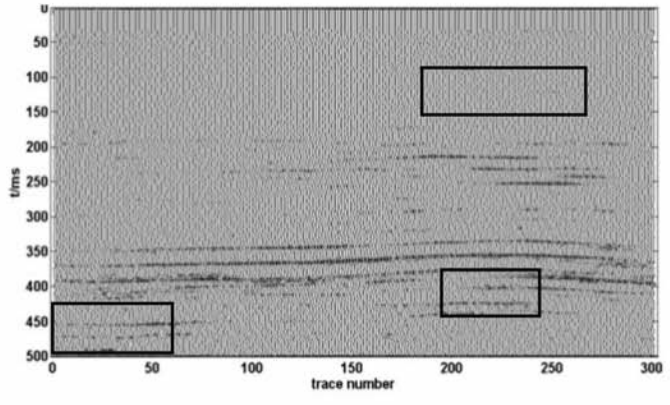

(b)

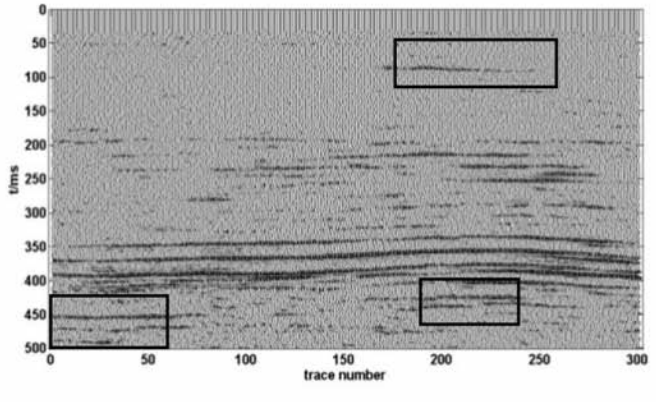

(c)

Fig. 8. Filtering results of real seismic data. (a) Original seismic data. (b) PWVD-TFPF result. (c) BJD-TFPF result.

Fig. 8 shows that in some areas, PWVD-TFPF almost eliminates-the signals, while the proposed method preserves them and the same phase axis can be seen clearly. The related indicators are recorded in Table 5. Because the original data contains noise and SNR cannot be calculated, we only show the SNR after filtering by two methods. Table 5 demonstrates the improvement of SNR with our method and Table 6 exhibits SNR for part of the data in three rectangular boxes.

Table 5. Comparisons of SNR of real seismic data.

TFD	SNR(dB) after filtering
PWVD	0.1833
BJD	6.5873

Table 6. Comparisons of SNR of three boxes in data.

SNR(dB) afi filteri / TFD	Box 1	Box2	Box 3
PWVD	-2.3714	0.3803	0.7076
BJD	4.1645	7.4349	7.3942

Fig. 8 plots several traces so that some same phase axes cannot be seen clearly. Thus, we extract traces in box 3 to show the specific real seismic data, depicted in Fig. 9. From Table 6 we can see that SNR is increased by about 6 dB in the three boxes, which means that our method preserves effective signal better and performs well in improving SNR.

As seen in Fig. 9, especially between the 450-460 ms record, the same phase axis is protected well by the proposed method. PWVD-TFPF reduces more noise than our method but its performance of preserving effective signal cannot meet the requirements of seismic data processing.

INFLUENTIAL FACTORS OF BJD-TFPF

Based on the previous results, BJD-TFPF can be applied in filtering seismic data. Yet, prior experiments used certain parameters. Practical seismic signals are complex and require us to determine–the relevant parameters. To apply our method well to real seismic data, we investigate different factors which can affect the filtering results. The prevalent parameters are time-domain window length (Wu et al., 2011; Li et al., 2009) and frequency-domain window length.

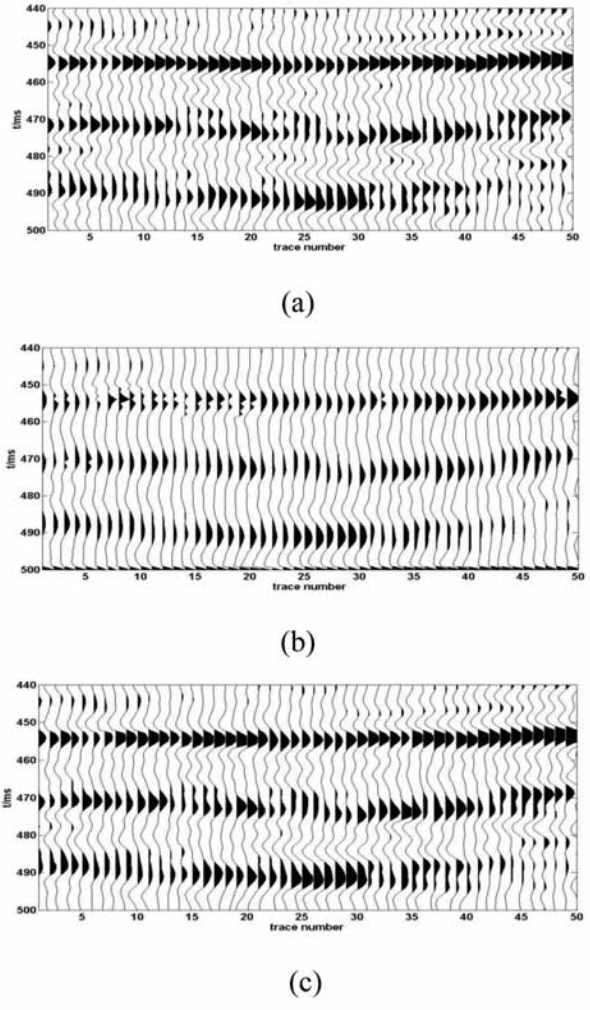

Fig. 9. Filtering results of box 3. (a) Original seismic data. (b) PWVD-TFPF result. (c) BJD-TFPF result.

According to experiments on the 40-trace synthetic signal, we summarize the rules of change and derive suitable parameters qualitatively.

Relationship between window length in the τ direction and SNR

We test on the 40-trace synthetic seismogram in Fig. 4(a). Random noise (mean = 0, variance = 0.25) is added and BJD-TFPF is applied to filter the signal. The result is shown in Table 7. We set the θ-domain window length to 9. According to the statistics in Table 7, we plot the relationship

between SNR and τ-domain window length curves in Fig. 10. We also use cubic curve to match the relationship. The results illustrate that the τ-domain window length is closely positively related to the filtering performance. From Fig. 10 we can see that SNR has improvements as the τ-domain window length increases when the θ-domain window length is fixed. The fitting curve also shows the increasing tendency.

Table 7. The relationship between the time-domain window length and SNR.

Window length	SNR(dB) before filtering	SNR(dB) after filtering	SNR(improvemen
3	-13.9940	-5.3099	8.6841
7	-13.9984	-4.7961	9.2023
11	-14.0754	-4.8231	9.2523
15	-13.9634	-4.5508	**9.4126**
19	-13.9786	-4.7095	9.2691
23	-13.9749	-4.4005	**9.5744**
27	-13.9742	-4.5872	9.3870
31	-13.9592	-4.5003	**9.4589**

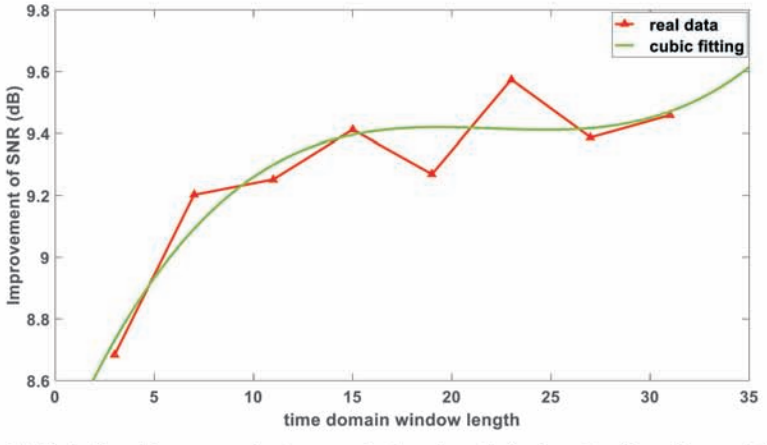

Fig. 10. Relationship curves between window length in the τ direction and SNR.

Relationship between window length in the θ direction and SNR

After discussing the τ-domain window length, we should consider the θ-domain window length as well. Except for the τ-domain window length of 9, the other parameters are the as in the previous section. The results are shown in Table 8.

As seen in Table 8, the effect of the θ-domain window length is complicated. With some short and long window lengths, BJD-TFPF performs better than with medium window length. According to the data, we

illustrate their relationship in Fig. 11 and apply cubic fitting to find their relationship. From Fig. 11 we can see that the improvement of SNR enhances at first and then goes down with increasing θ-domain window length. The matching curve shows the same tendency as well. The best result appears at window length 15 compared with window 23 in the τ-domain.

Table 8. Relationship between the frequency-domain window length and SNR.

Window length	SNR(dB) before filtering	SNR(dB) after filtering	SNR(improvement)
3	-14.0282	-8.6424	5.3858
7	-14.0035	-5.4641	8.5394
11	-14.0124	-4.0953	9.9171
15	-13.9898	-3.7045	**10.2853**
19	-13.9723	-4.1357	9.8366
23	-14.0159	-4.1286	9.8873
27	-14.0379	-3.9012	**10.1367**
31	-13.9796	-3.7574	**10.2222**

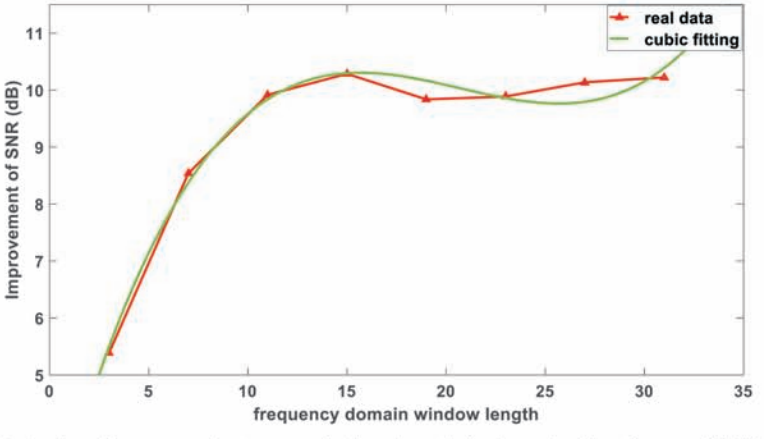

Fig. 11. Relationship curves between window length in the θ direction and SNR.

From the results above, when we need to apply BJD-TFPF to real seismic data, we can choose a τ-domain window length of between 23 and 31 and a θ-domain window length of between 27 and 31, or of 15.

CONCLUSION

In this paper, we proposed the BJD-TFPF method to solve the noise problem in seismic data. The results of experiments on multicomponent

signals, synthetic seismic data and real data show that BJD preserves the signal better at the margins and provides improvement in SNR. We also discussed the factors of BJD-TFPF that make it more practical and convenient to apply to seismic field data. However, only a qualitative relationship is derived and the quantitative relationship needs further research. Furthermore, other comparisons need to be studied to improve our results and develop our method in the future.

ACKNOWLEDGEMENTS

This work is supported by the National Natural Science Foundation of China (61571096, 41274127, 41301460) and the Center for Information Geoscience. The authors are grateful to Dehui Kong, Jiangyang Li and Lingma Sun for their constructive help and data.

REFERENCES

Arnold, M.J., Roessgen, M. and Boashash B., 1993. Signal filtering using frequency encoding and the time-frequency plane. Conf. Rec. 27th Asilomar Conf. Signals, Systems Comput. IEEE, 2: 1459-1463

Boashash, B. and Mesbah, M., 2004. Signal enhancement by time–frequency peak filtering. IEEE Transact. Signal Process., 52: 929-937

Ivanovic,V.N., Daković, M. and Stankovic, L., 2003. Performance of quadratic time-frequency distributions as instantaneous frequency estimators. IEEE Transact. Signal Process., 51: 77-89.

Jones, I.F. and Levy, S., 1987. Signal-to-noise ratio enhancement in multichannel seismic data via the Karhunen-Loéve transform. Geophys. Prosp., 35: 12-32.

Li, Y., Lin, H.B., Yang, B.J., Wu, N., Li, S.K. and Gao, H., 2009. The influence of limited linearization of time window on TFPT under the strong noise background. Chin. J. Geophys., 5: 1899-1906.

Li, Y., Yang, B.J., Lin, H.B., Ma, H.T. and Nie P.F., 2013. Suppression of strong random noise in seismic data by using time-frequency peak filtering. Sci. China (Earth Sci.), 7: 1200-1208.

Lin, H.B., Li, Y., Ma, H.T., Yang, B.J. and Dai, J., 2014. Matching-pursuit-based spatial-trace time-frequency peak filtering for seismic random noise attenuation. IEEE Geosci. Remote Sens. Lett., 12: 394-398.

Lin, H.B., Li, Y. and Xu, X.C., 2011. Segmenting time-frequency peak filtering method to attenuation of seismic random noise. Chin. J. Geophys., 54: 1358-1366.

Lin, H.B., Li, Y., Yang, B.J. and Ma, H.T., 2013. Random denoising and signal nonlinearity approach by time-frequency peak filtering using weighted frequency reassignment. Geophysics, 78 (6): V229-V237.

Lin, H.B., Li, Y., Yang, B.J., Ma, H.T. and Zhang, C., 2013. Seismic random noise elimination by adaptive time-frequency peak filtering IEEE Geoscience & Remote Sensing Letters **11** (1) 337-341.

Liu, Y.P., Dang, B., Li, Y. and Lin, H.B., 2014. Local spatiotemporal time–frequency peak filtering method for seismic random noise reduction. J. Appl. Geophys., 111: 76-85

Liu, Y.P., Li, Y., Lin, H.B. and Ma, H.T., 2014. An amplitude-preserved time–frequency peak filtering based on empirical mode decomposition for seismic random noise reduction. IEEE Geoscience & Remote Sensing Letters, **11** (5), 896-900.

Liu, Y.P., Li, Y., Nie, P.F. and Zeng, Q., 2013. Spatiotemporal time-frequency peak filtering method for seismic random noise reduction. IEEE Geosci. Remote Sens. Lett, 10: 756-760.

Mesbah, M. and Boashash, B., 2001. Reduced bias time-frequency peak filtering. 6th Internat. Symp. Signal Process. Applicat., IEEE, 1: 327-330.

Tian, Y. and Li, Y., 2014. Parabolic-trace time–frequency peak filtering for seismic random noise attenuation. IEEE Geosci. Remote Sens. Lett., 11: 158-162.

Wang, Z.G., Gao, J.H., Zhou, Q.B., Li, K.X. and Peng, J.G., 2013. A new extension of seismic instantaneous frequency using a fractional time derivative. J. Appl. Geophys., 98: 176-181.

White, R.E., 1984. Signal and noise estimation from seismic reflection data using spectral coherence methods. Proc. IEEE, 72: 1340-1356.

Wu, N., Li, Y. and Yang, B.J., 2011. Noise Attenuation for 2-D seismic data by radial-trace time-frequency peak filtering. IEEE Geosci. Remote Sens. Lett., 8: 874-878.

Xiong, M.J., Li, Y. and Wu, N., 2014. Random-noise attenuation for seismic data by local parallel radial-trace TFPF. IEEE Transact. Geosci. Remote Sens., 52: 4025-4031.

Zhang, C, Lin, H.B., Li, Y. and Yang, B.J., 2013. Seismic random noise attenuation by time-frequency peak filtering based on joint time-frequency distribution. Compt. Rendus – Géosci., 345: 383-391.